

Onset of Maternal Arterial Blood Flow and Placental Oxidative Stress

A Possible Factor in Human Early Pregnancy Failure

Eric Jauniaux,* Adrian L. Watson,[†]
Joanne Hempstock,[†] Yi-Ping Bao,[†]
Jeremy N. Skepper,[†] and Graham J. Burton[†]

From the Academic Department of Obstetrics and Gynaecology,*
University College London, London; and the Department of
Anatomy,[†] University of Cambridge, Cambridge, United Kingdom

The aim was to measure changes in the oxygen tension within the human placenta associated with onset of the maternal arterial circulation at the end of the first trimester of pregnancy, and the impact on placental tissues. Using a multiparameter probe we established that the oxygen tension rises steeply from <20 mmHg at 8 weeks of gestation to >50 mmHg at 12 weeks. This rise coincides with morphological changes in the uterine arteries that allow free flow of maternal blood into the placenta, and is associated with increases in the mRNA concentrations and activities of the antioxidant enzymes catalase, glutathione peroxidase, and manganese and copper/zinc superoxide dismutase within placental tissues. Between 8 to 9 weeks there is a sharp peak of expression of the inducible form of heat shock protein 70, formation of nitrotyrosine residues, and derangement of the mitochondrial cristae within the syncytiotrophoblast. We conclude that a burst of oxidative stress occurs in the normal placenta as the maternal circulation is established. We speculate that this may serve a physiological role in stimulating normal placental differentiation, but may also be a factor in the pathogenesis of pre-eclampsia and early pregnancy failure if antioxidant defenses are depleted. (*Am J Pathol* 2000, 157:2111–2122)

One of the key requirements for a successful pregnancy is adequate materno-fetal exchange. The placenta has evolved to meet this requirement, and provides an extensive and intimate interface between the maternal and fetal blood streams. In the human this is achieved through the elaboration of a series of fetal villous trees that are bathed directly by maternal blood circulating in the intervillous space.¹ For many years the general assumption has been that the maternal circulation is established inside the placenta shortly after implantation

through the invasion of endometrial vessels by the fetal trophoblast.² This view was first challenged by Hustin and colleagues^{3,4} who argued on the basis of anatomical and ultrasound findings that significant maternal blood flow does not occur until 12 weeks of gestation. These findings have been criticized as reflecting *ex vivo* artifacts and lack of instrument sensitivity, but if proven the claim would radically alter our understanding of the nutritional supply to the developing human embryo, and of the pathophysiology of early pregnancy disorders. Not surprisingly therefore, the stage of pregnancy at which the maternal arterial circulation to the placenta becomes fully established has recently become a highly contentious issue.^{5–8}

Attempts to address the question using Doppler ultrasound techniques have obtained conflicting results,^{8–10} and it is clear that the debate will not be resolved while discussion focuses on issues such as the relative sensitivities of ultrasound equipment or the precise localization of recordings from within the placenta. We have therefore adopted a physiological approach. One of the major implications of the new theory is that the oxygen tension within the early fetoplacental unit will be considerably lower than previously anticipated, rising with the onset of maternal blood flow. We tested this prediction by measuring the oxygen concentration within the placental intervillous space with a highly accurate and sensitive multiparameter probe at different gestational ages.

Aerobic metabolism is inextricably associated with the generation of reactive oxygen species, and the rate of their formation is proportional to the prevailing oxygen tension.¹¹ These species are potentially extremely hazardous and so a complex system of antioxidant defenses has evolved to meet this challenge (Figure 1). To gain further evidence of the oxygen concentration at the cellular level we therefore assayed the mRNA concentration and activity of the principal antioxidant enzymes catalase, glutathione peroxidase (GPX), and copper/zinc and

Supported by a grant from the Medical Research Council (G9701485), and University College London Hospital Special Trustees, London, United Kingdom.

Accepted for publication September 11, 2000.

Address reprint requests to Dr. G. J. Burton, Department of Anatomy, University of Cambridge, Downing St., Cambridge CB2 3DY, UK. E-mail: gjb2@cam.ac.uk.

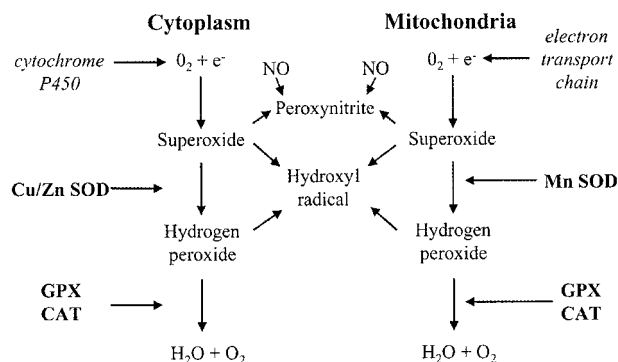


Figure 1. Oxygen-free radicals are produced through the leakage of electrons from electron transport chains in the mitochondria and endoplasmic reticulum on to molecular oxygen. The superoxide anion generated is not freely diffusible through cell membranes and must be dismutated *in situ* by either Cu/Zn or Mn SOD. Although H₂O₂ is not a free radical it can react with O₂⁻ to form the extremely reactive hydroxyl radical. Catalase and GPX must therefore operate in concert with the SODs to keep concentrations at physiological levels.

manganese superoxide dismutases (SOD) within placental tissues at different ages.

If the oxygen concentration fluctuates too rapidly or rises too high then cellular antioxidant defenses can become overwhelmed, resulting in oxidative stress. In these circumstances indiscriminate damage to proteins, lipids, and DNA severely impairs normal cellular functions, and may even lead to cell death. We have previously found the syncytiotrophoblastic layer of the early placenta to be exquisitely sensitive to rapidly rising oxygen tensions *in vitro*, undergoing selective degeneration.¹² We therefore sought evidence of oxidative stress in the trophoblast associated with changes in the maternal circulation to the placenta *in vivo*. This was achieved immunohistochemically by monitoring expression of the inducible form of heat shock protein 70 (Hsp 70i), a recognized marker of oxidative stress in other systems,¹³ and the formation of nitrotyrosine residues at different gestational ages. We also assessed mitochondrial morphology, for as these organelles are the principal site of free radical generation they are particularly susceptible to increases in oxygen tension.¹²

Materials and Methods

Cases

Measurement of intrauterine gases was performed in 30 healthy women undergoing surgical termination of pregnancy under general anesthesia for psychosocial reasons at 7 to 16 weeks of gestation. All women gave their written informed consent to participate in this study which had been approved by the University College London Hospitals Committee on the Ethics of Human Research.

Oxygen Measurements

The Paratrend 7 monitoring system with automated sensor calibration (Diametrics Medical, St. Paul, MN) contains a sterile electrochemical sensor (Clark electrode)

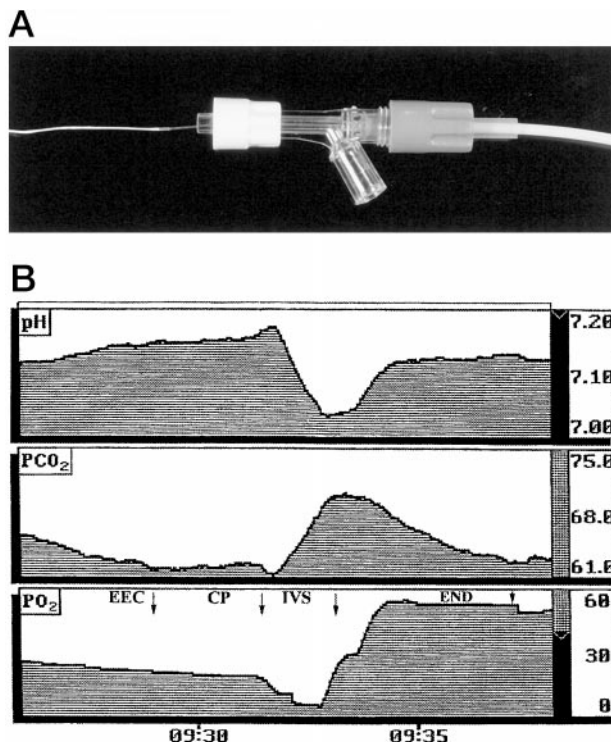


Figure 2. A: The Paratrend multiparameter probe has a diameter of 0.5 mm and contains PO₂, PCO₂, pH, and temperature sensors. **B:** Sample output from the Paratrend probe illustrating the stability of the pH, PCO₂, and PO₂ measurements obtained. In this example, at 60 days of gestation, the probe was first introduced into the extra-embryonic coelom (EEC), and was then withdrawn through the placental chorionic plate (CP) into the placental intervillous space (IVS) and then finally into the endometrium (END) underlying the placenta. The probe rapidly stabilizes in each new environment, and thereafter there is a slight downward trend in the oxygen measurements. This most likely reflects oxygen consumption by the Clark electrode depleting the concentration in the immediate vicinity of the probe.

for measuring oxygen concentrations (Figure 2). It is calibrated with three precision gases supplied by the manufacturer, and has a range of 0 to 120 mmHg and 95% confidence intervals of ± 1 mmHg. The 0 to 90% response time is <150 seconds.

The probe was introduced through an 18-G needle positioned under continuous ultrasound guidance longitudinally inside the placental intervillous space, and subsequently in the uterine decidua underlying the placental basal plate.¹⁴ After a period of 2 to 3 minutes for stabilization, five measurements were taken at 1-minute intervals at each site and the mean value was recorded (Figure 2).

Maternal peripheral-arterial blood saturation was evaluated continuously by pulse oximetry with a probe applied to a finger.

Collection and Processing of Experimental Tissue

After the probe measurements, placental tissue was obtained under ultrasound guidance using a chorionic villous sampling procedure to minimize tissue damage and contamination. Villous tissue was immediately washed in ice-cold saline and dissected away from associated

blood clots, membranes, and maternal tissues. Samples were either snap-frozen in liquid N₂ and stored at -80°C, fixed immediately for 2 hours at room temperature in 4% formaldehyde in 0.1 mol/L Pipes buffer (pH 7.0), or fixed in 2% glutaraldehyde in 0.1 mol/L Pipes buffer.

Anti-Oxidant Enzyme Activity Assays

Frozen villous tissue was thawed on ice and 100 mg wet weight dissected away. Tissue was homogenized in 50 mmol/L sodium phosphate buffer (pH 7.4), 1 mmol/L phenylmethylsulfonyl fluoride, 0.05% Triton X-100, and a soluble fraction component was prepared by centrifugation at 20,000 × *g* for 30 minutes at 4°C. The supernatant was removed and the pelleted material washed using the phosphate buffer. After further centrifugation the two supernatants were combined, mixed, and assayed immediately. Protein concentrations were determined using the Lowry method and all concentrations adjusted to 2 mg/ml. All assays were repeated 12 times and the mean recorded. Assays of antioxidant activities in the pelleted material indicated that a maximum of 5% of total activities was retained in this fraction.

Total SOD Activity

The final assay mixture comprised the following: 65 mmol/L sodium phosphate (pH 7.8), 25 μmol/L nitroblue tetrazolium, 100 μmol/L hypoxanthine, 0.02 U/ml xanthine oxidase, and 1, 2, 5, or 10 μg of homogenate protein. The reaction was allowed to equilibrate at 37°C for 30 seconds and then absorbance change at 570 nm was monitored for 2 minutes. Relative activities are expressed as ΔOD/minutes/mg protein.

Catalase Activity

The final assay mixture contained 50 mmol/L sodium phosphate (pH 7.0), 12 mmol/L hydrogen peroxide and 2, 5, or 10 μg of homogenate protein. The disappearance of hydrogen peroxide was followed spectrophotometrically at 230 nm at 25°C. Rates are expressed as ΔOD/minutes/mg protein. The addition of catalase inhibitor 3-amino-1,2,4-triazole, pre-incubated for 2 minutes with homogenate at 25°C, resulted in rates which barely registered on the spectrophotometric output.

GPX Activity

Cellular activity was assayed using a kit (Calbiochem-Novabiochem). In brief, the final reaction mixture comprised the following assay buffer (pH 7.6) 0.2 mmol/L NADPH, 1 mmol/L glutathione, 0.4 U/ml glutathione reductase, 0.22 mmol/L *tert*-butyl hydroperoxide and 5, 10, or 20 μg homogenate protein. After a pre-incubation of 30 seconds, utilization of NADPH at 37°C was followed spectrophotometrically (340 nm) for 2 minutes, and rates are expressed as ΔOD/minutes/mg protein. Two types of

control blanks were performed using water instead of homogenate or water instead of *tert*-butyl hydroperoxide.

Reduced Glutathione Assay

Concentrations were determined using a kit (Calbiochem-Novabiochem, Nottingham, UK). Placental tissue was minced in ice-cold 5% metaphosphoric acid, and homogenized using a tight-fitting Teflon pestle. The homogenate was centrifuged at 3,000 × *g* for 10 minutes at 4°C. The final assay mixture contained: assay buffer (200 mmol/L potassium phosphate (pH 7.8) containing 0.2 mmol/L diethylene triamine penta-acetic acid, 0.025% Lubrol), 0.6 mmol/L chromogenic reagent, 1.5% w/v sodium hydroxide, and 5, 10, or 20 μl of homogenate supernatant. The reaction mixture was incubated at 25°C for 10 minutes in the dark and the absorbance then measured at 400 nm. The assay was made quantitative using a standard curve with reduced glutathione concentrations between 5 and 100 μmol/L. All calculations for glutathione concentration were performed after subtraction of readings for buffer controls.

Northern Blots

Total RNA was prepared from 11 samples ranging in gestational age from 7 to 14 weeks using Trizol reagent (Gibco BRL, Paisley, UK) according to the manufacturer's protocol. Samples of RNA (15 μg) were electrophoresed on a 0.8% formaldehyde/agarose gel and transferred onto positively charged nylon membrane (Roche Molecular Biochemicals, Lewes, UK). The cDNA of the antioxidant enzymes catalase, GPX, Cu/ZnSOD, and MnSOD were subcloned from PCR Blunt (Invitrogen, Groningen, The Netherlands) into pGEM-4Z vector (Pharmacia Biotech, Uppsala, Sweden). Blots were hybridized with the ³²P-labeled cDNA probes separately. The plasmids were prepared with a Plasmid Isolation Kit (Qiagen, Crawley, UK). An 18S ribosomal RNA probe was used to normalize loading. The membranes, which were washed to high stringency, were put into a phosphor-imaging cassette with a storage screen. The image was detected using the Storm Imaging System (Molecular Dynamics, Uppsala, Sweden).

Immunohistochemical Staining of Inducible Hsp 70 and Nitrotyrosines

Tissue fixed in paraformaldehyde was embedded in paraffin wax and sectioned at 5 μm. Sections were dewaxed in xylene, rehydrated, treated with 0.1% H₂O₂ for 30 minutes, rinsed in phosphate-buffered saline (PBS), blocked for 20 minutes in 1.5% goat serum/PBS, and incubated for 2 hours at room temperature with the primary antibodies; rabbit anti-nitrotyrosine (2 μg/ml; Chemicon, Temecula, CA), and rabbit polyclonal anti-Hsp 70 inducible form (1 μg/ml; StressGen, York, UK). Further processing for colorimetric detection was according to the instructions for the Vectastain ABC kit (Vector Laboratories,

Burlingame, CA). Negative controls were performed alongside substituting nonimmune rabbit serum for primary antibody against Hsp 70i. For nitrotyrosines the primary antibody was pre-incubated with 10 mmol/L 3-nitro-L-tyrosine overnight.

For quantification of Hsp 70i expression adjacent sections were incubated with a fluorescein isothiocyanate-labeled secondary anti-rabbit antibody. After blinding for gestational age they were viewed with a Leica true confocal scanner-Windows NT confocal microscope using a $\times 40$ objective, a 488-nm excitation wavelength and a 530/30 band-pass filter for emitted light. The pinhole setting was 1 Airey-disk equivalent. Laser power, the acousto-optic threshold filter setting, and detection photomultiplier tube gain remained constant throughout. Under these conditions the thickness of the confocal optical section is $\sim 0.5 \mu\text{m}$. This was positioned within the thickness of the $5\text{-}\mu\text{m}$ physical section, thus eliminating the effects of variation in tissue section thickness. To avoid bleaching, five randomly selected fields of view per section were rapidly saved for later analysis. Quantitative assessment was achieved using the Leica true confocal scanner-Windows NT quantification software to assess mean fluorescent intensity measurements along randomly positioned lines projected through the longest axis of the syncytiotrophoblast or the stromal core. The mean of these values was then recorded for each placenta.

Electron Microscopy

Samples were secondary fixed in 1% osmium tetroxide in Pipes buffer for 1 hour at room temperature and embedded in Araldite epoxy resin. Ultra-thin sections (150 nm) were counterstained with uranyl acetate followed by lead citrate, and viewed using a Philips CM100 microscope (FEI/Philips, Eindhoven, The Netherlands). For each placenta at least 20 mitochondria were selected at random by viewing areas of syncytiotrophoblast immediately adjacent to grid bars, and the volume fraction of the intracristal space was estimated by point counting.¹²

Statistics

The data were analyzed with a statistics package (Statview, SAS Institute, Cary, NC), and results were considered statistically significant at $P < 0.05$. Relationships between variables were first tested by correlation analysis, and if significant, were explored further using bivariate scatterplots and the LOWESS (locally weighted scatterplot smoother) technique.

Results

Manipulation of the Probe

The tip of the probe could be identified at all times using ultrasound, allowing for accurate positioning of the sensors. No acute complication was associated with the use of the Paratrend probe in the placenta or decidua. In particular, insertion of the needle and sensor did not

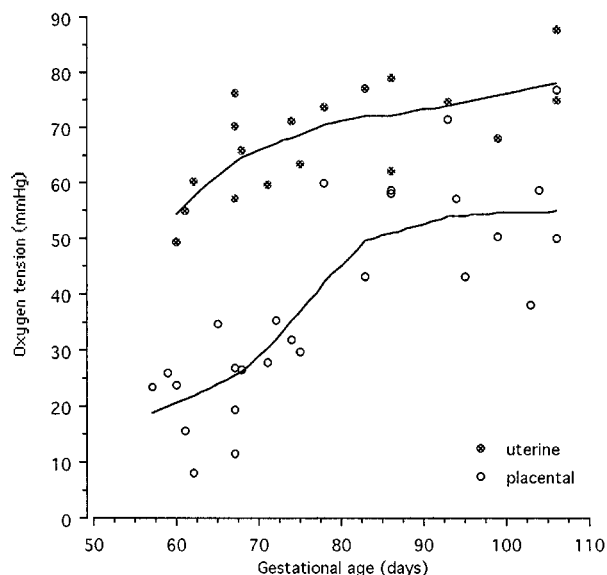


Figure 3. Bivariate scattergram of the placental and uterine PO_2 measurements against gestational age. The curves were fitted with the LOWESS technique with a tension of 60. The PO_2 in the placenta rises steeply between 10 to 12 weeks, reflecting the onset of free maternal blood flow into the intervillous space.

appear to damage the tissues as shown by an absence of bleeding and/or any echographic signs of hematoma. The probe however proved to be delicate, and was damaged on four occasions when entering the placenta and on a further eight when moving from the placenta into the decidua.

Once inserted into the area of interest the measurements stabilized rapidly. The mean coefficient of variation ($\text{SD}/\text{mean} \times 100$) of the measurements during the 5 to 8 minutes of monitoring was 3.6% for the placenta, and 3.3% for the decidua. For technical reasons relating to the size of the probe, and the size and delicacy of the placental tissues, it was not possible to obtain reliable measurements before 8 weeks of gestation.

Maternal arterial blood oxygen saturation monitored by the finger-tip clip remained constant during the procedure, with values ranging between 96 and 99% (mean, 97.5%; $\text{SD} \pm 0.7$), confirming that the patients were well ventilated throughout.

Probe Measurements

There was a highly significant positive correlation between the mean PO_2 recorded within the intervillous space and the gestational age ($n = 26$, $r = 0.80$, $P < 0.001$). However, a bivariate scattergram illustrated that the data fell into two sets, an early set including weeks 7 to 11 and a later set including weeks 12 to 15. If each data set was analyzed separately no correlation existed ($n = 14$, $r = 0.46$, $P > 0.05$ and $n = 12$, $r = 0.02$, $P > 0.05$ for the early and late values, respectively). In view of this finding a sigmoid curve was fitted to the data using the LOWESS technique with a tension of 60 (Figure 3). This analysis indicated that the oxygen tension within the placenta rises steeply during weeks 10 to 12 of pregnancy.

Table 1. Correlation Coefficients for Placental Anti-Oxidants with Gestational Age and the Oxygen Tension Measured within the Intervillous Space

	Gestational age	Intervillous PO ₂
Glutathione peroxidase activity	0.763 (<i>n</i> = 19, <i>P</i> < 0.001)	0.784 (<i>n</i> = 18, <i>P</i> < 0.001)
Reduced glutathione concentration	0.536 (<i>n</i> = 20, <i>P</i> = 0.014)	0.408 (<i>n</i> = 19, <i>P</i> = 0.083)
Catalase activity	0.544 (<i>n</i> = 20, <i>P</i> = 0.012)	0.532 (<i>n</i> = 19, <i>P</i> = 0.018)
Total SOD activity	0.392 (<i>n</i> = 20, <i>P</i> = 0.088)	0.491 (<i>n</i> = 19, <i>P</i> = 0.032)

The PO₂ in the endometrium beneath the placenta also correlated with gestational age (*n* = 18, *r* = 0.68, *P* = 0.001). These values increased in a more linear manner and were considerably higher than those measured within the placenta. Consequently an oxygen gradient always existed between the endometrium and the intervillous space, but the magnitude of this declined with increasing gestational age (Figure 3). This pattern confirms that more maternal blood enters the placenta from the endometrium as pregnancy advances rather than there being significant changes in maternal oxygenation.

Antioxidant Defenses

GPX activity within the placental tissues showed a strong positive correlation with gestational age (Table 1), with activity increasing slowly until the end of the tenth week and faster thereafter (Figure 4a). A similar pattern was observed in the concentration of reduced glutathione although these data showed considerable scatter at early ages (Table 1 and Figure 4b). Catalase activity also correlated with gestational age (Table 1), but in this case activity rose steadily and then plateaued at ~12 weeks (Figure 4c). Although total SOD activity demonstrated a trend toward increased activity with age, this failed to reach statistical significance (Table 1 and Figure 4d).

The activities of the antioxidant enzymes showed equally strong correlations with the oxygen tension measured in the intervillous space (Table 1). However, although the concentration of reduced glutathione seemed to increase with rising oxygen tensions this trend failed to reach statistical significance.

mRNA Concentrations

A representative blot is shown in Figure 5. For statistical analysis the samples were divided into two groups according to gestational age; before and after 10 weeks, respectively. Mean gestational age in the first group was 56 days (*n* = 5, SD = 9.3) and in the second group was 92.7 days (*n* = 6, SD = 6.7). Densitometry readings relative to 18S ribosomal RNA revealed that the mRNA concentrations for catalase, Cu/ZnSOD and GPX all increased with gestational age (*t* = 2.51, *P* = 0.033; *t* = 2.60, *P* = 0.029 and *t* = 2.21, *P* = 0.05, respectively). Two bands were observed for MnSOD at 1 kb and 4 kb. No change was observed in the former, and although it appeared that there was an increase in the latter the

difference failed to reach statistical significance (*t* = 1.56, *P* = 0.15).

Inducible Hsp 70 Expression

Expression of Hsp 70i was extremely low in the earliest 6- to 7-week tissue (Figure 6a), but showed a marked increase in 8- to 9-week villi with particularly strong immunolabeling in the syncytiotrophoblast and endothelial cells (Figure 6b). Thereafter expression seemed to decline in tissues of older gestational age and became uniform between the different cell types (Figure 6c). All negative controls demonstrated minimal background staining (Figure 6d). Two runs of the quantification procedure were performed because of the physical limitations imposed by immunolabeling and viewing a large number of sections under the same conditions. Each run contained a complete range of ages, although the second concentrated on samples from 7 to 10 weeks. The data for each run are therefore internally consistent, but the two runs are not strictly comparable because of possible variations in labeling conditions or microscope laser power. The two data sets are therefore plotted as scattergrams (Figure 7). In each case low levels of expression were observed in the trophoblast of the earliest samples. However, there was a sharp peak of fluorescence intensity in samples from 8 to 9 weeks of gestational age, with later samples showing intermediate levels of expression. Values for the stroma were consistently lower than those for the trophoblast layer, but followed a similar pattern.

Detection of Nitrotyrosine Residues

A generally similar pattern of immunolabeling was observed for nitrotyrosine residues as for Hsp 70i, with a marked contrast between gestational ages. Residues were virtually undetectable in the earliest 6- to 7-week tissues, were increased throughout the 8- to 9-week villi, but reduced again at 10 to 12 weeks (Figure 6, e-g). Controls using the pre-incubated primary antibody displayed minimal staining (Figure 6h).

Mitochondrial Morphology

In the 6-week tissue the mitochondrial profiles were smoothly oval or circular in shape, and the cristae were clearly visible as a series of classically arranged interdig-

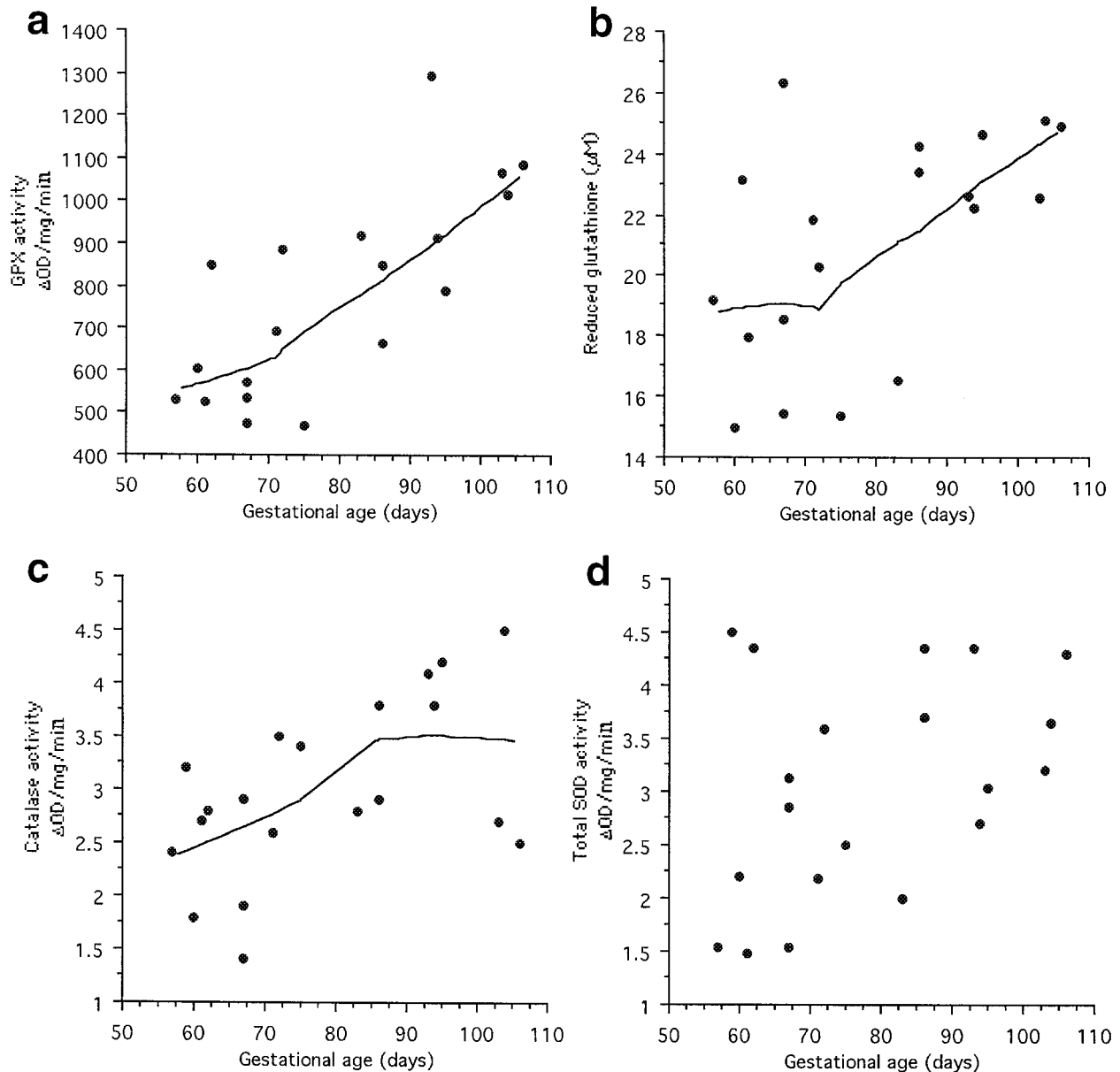
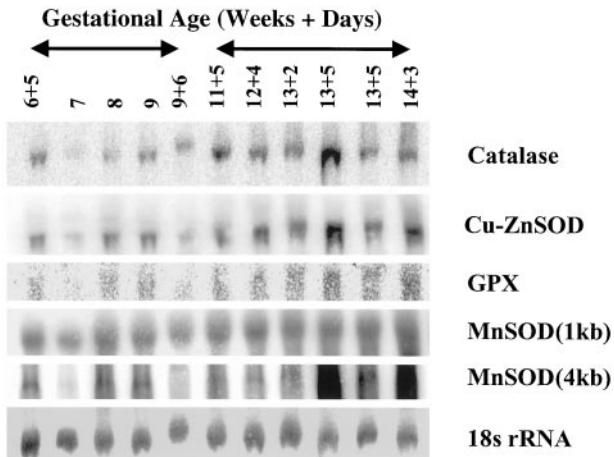


Figure 4. Bivariate scattergrams of the placental activities of the antioxidant enzymes and the concentration of reduced glutathione against gestational age. All showed a significant correlation except for total SOD activity (Table 1), and lines were fitted using the LOWESS technique. **a:** GPX activity, LOWESS tension 70. **b:** Reduced glutathione concentration, LOWESS tension 70. **c:** Catalase activity, LOWESS tension 75. **d:** Total SOD activity.

itating folds. The matrix was moderately electron-dense (Figure 8a). At 9 to 10 weeks the appearances were very different. The profiles appeared smaller in area, and more irregular in outline. Fewer cristae were visible, and often these were in the form of a single circle within the matrix. The intracristal space within the cristae was substantially dilated (Figure 8b). By 12 to 14 weeks cristae could be clearly defined again although they were more irregularly arranged than in the early specimens (Figure 8c). Quantification confirmed that the percentage volume of the organelles occupied by intracristal space showed an initial rise coinciding with the Hsp 70 expression, and a subsequent decline as gestational age increased (Figure 8d). A second order polynomial regression showed these changes to be statistically significant ($F = 3.94, P < 0.05$).

Discussion

The data presented here provide conclusive evidence that the oxygen tension within the human placenta increases rapidly at the end of the first trimester of pregnancy. The increase cannot be explained by vasospasm or similar artifact induced selectively in the early cases by the maternal anesthesia or introduction of the probe as it is matched by rises in the mRNA concentrations and activities of the antioxidant enzymes. Antioxidant gene expression is responsive to the prevailing oxygen tension,^{15,16} but there will be an inevitable delay while transcription and translation take place. Hence, the antioxidant data provide evidence of the oxygen tension at the cellular level during the period immediately preceding removal of the tissue.



Northern blot analysis of total RNA isolated from placental villi of different gestational ages.

Figure 5. Representative Northern blots for the antioxidant enzymes. A significant increase in expression with gestational age was observed for catalase, GPX, and Cu/ZnSOD but not for MnSOD.

Our data are consistent with classical morphological descriptions of early placental development. These state that during implantation the trophoblast invades into capillaries and veins within the superficial endometrium, and that maternal erythrocytes are present in the precursors of the intervillous space. This represents a capillary circulation only, however, and direct connections between the spiral arteries and the intervillous space cannot be observed before the ninth week of gestation.^{17,18} Before that stage the distal segments of the arteries are occluded by aggregates of cytotrophoblast cells derived from the developing cytotrophoblastic shell and the villous cell columns.^{4,19} Arterial communication with the enlarging intervillous space is therefore restricted to a network of narrow intercellular spaces, ensuring that any flow is sluggish or restricted to a plasma filtrate. Both these phenomena could account for the low oxygen tension measured within the placenta on account of the small quantity of oxygen they deliver. The loosening of some of the arterial plugs at around 10 weeks allows maternal blood to enter the intervillous space more freely, accounting for the change in flow patterns detected with Doppler ultrasound at the end of the first trimester.^{7,9} As

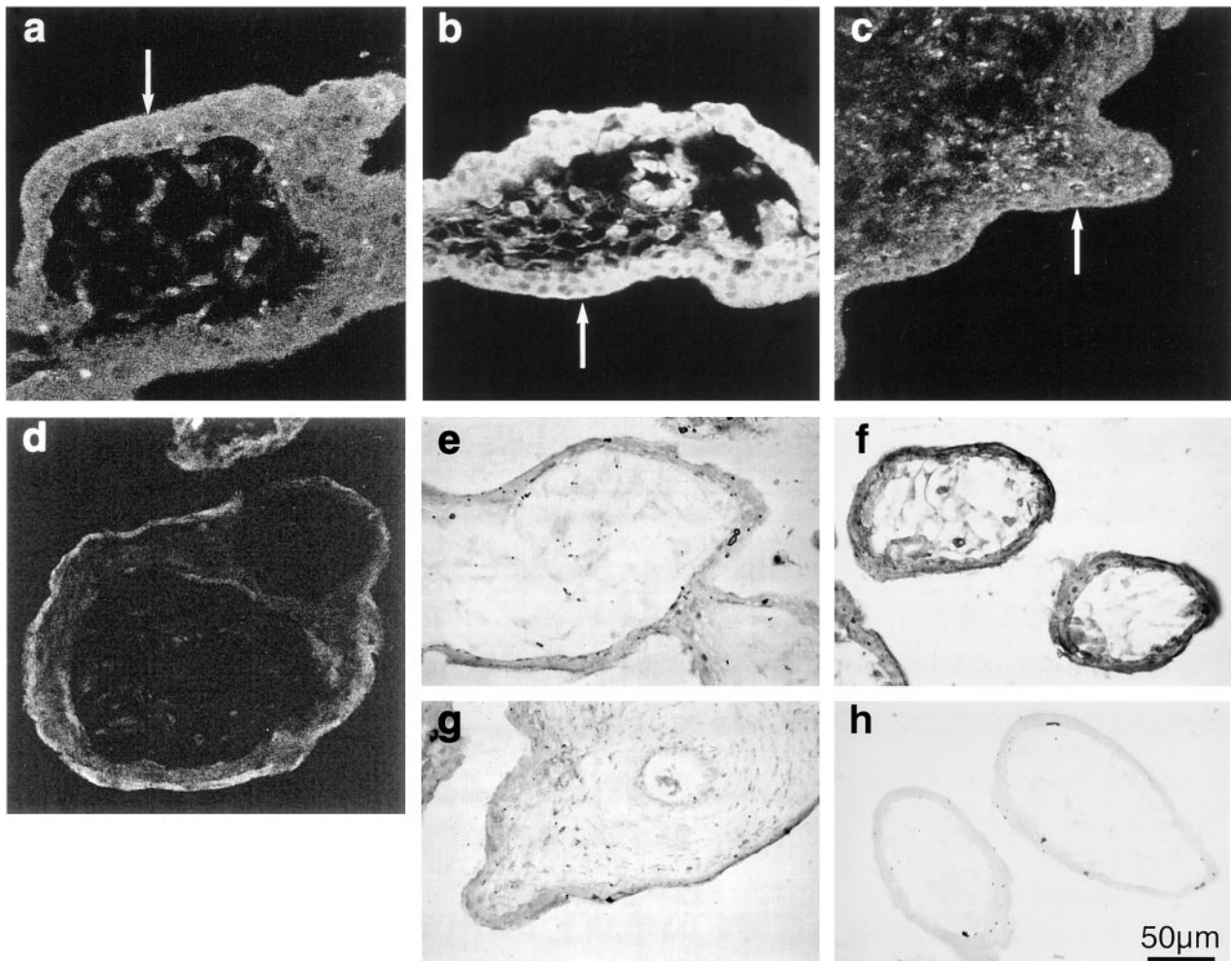


Figure 6. Immunohistochemical localization of inducible Hsp 70 expression using fluorescein isothiocyanate-labeled secondary antibodies in villi at 6 weeks (a), 9 weeks (b), and 13 weeks gestational age (c). d: Negative control and nitrotyrosines with chromogenic substrate at 6 weeks (e), 9 weeks (f), and 13 weeks gestational age (g). h: Negative control. There is strong immunolabeling for both at 9 weeks, particularly in the syncytiotrophoblast (arrows).

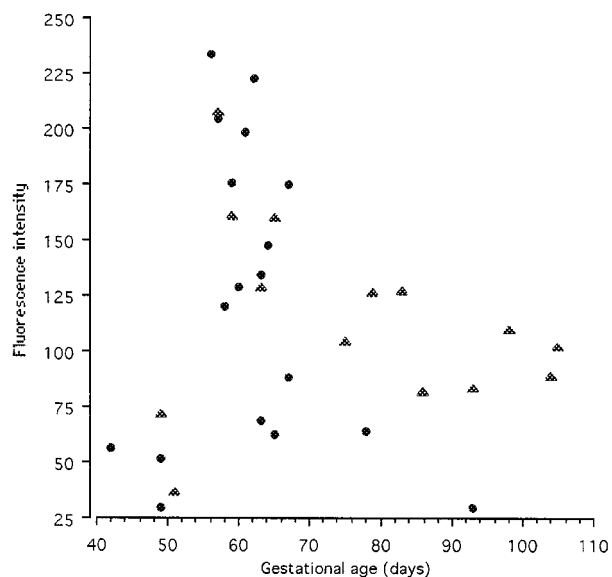


Figure 7. Scattergram of the mean fluorescence intensity of inducible Hsp 70 expression in the syncytiotrophoblast at different gestational ages. Two separate runs were performed, indicated by the symbols. The sections in each run were all immunolabeled together and viewed on the same day with the confocal microscope settings remaining constant. Both runs display a peak of Hsp 70i expression at 8 to 9 weeks, indicating a period of oxidative stress.

a result the total quantity of oxygen delivered to the placenta will rise, leading to an increase in the PO_2 within the intervillous space.

Although it is clear the steepest rise in intervillous PO_2 occurs at around the tenth week it is not possible to identify precisely when the rise begins. Before 8 weeks the placenta proved too small to accommodate the probe so earlier data are not available. It is likely however that the onset of the circulation is a gradual event, and that considerable individual variation occurs between placentas. Aerobic metabolism is inevitably associated with the generation of free radical species, principally through the transfer of single electrons to molecular oxygen during their passage along the mitochondrial electron-transport chain. This occurs at the level of either NADH dehydrogenase or coenzyme Q, and results in the formation of the superoxide anion, $O_2^{\cdot-}$. The rate of formation is proportional to the prevailing oxygen concentration,¹¹ and a series of enzymatic antioxidant defenses have evolved to quench this and other resultant radicals. The manganese form of SOD located within the mitochondrial matrix readily dismutates $O_2^{\cdot-}$ to hydrogen peroxide, H_2O_2 (Figure 1). Although not a radical, H_2O_2 can react with free ferrous iron to yield the highly reactive hydroxyl radical, HO^{\cdot} . It is therefore important that H_2O_2 is maintained at physiological concentrations, and the enzymes GPX and catalase detoxify it to oxygen and water. GPX is located both within the mitochondrial matrix and the cytoplasm, whereas catalase is restricted primarily to peroxisomes. GPX uses reduced glutathione as a substrate, and so the intracellular pool of this tripeptide represents an important redox buffer. Indeed, it has been estimated that the pool contains >90% of all cellular reducing equivalents.²⁰ Superoxide anions may also be formed within the

endoplasmic reticulum, and here the Cu/Zn form of SOD is the first enzyme in the detoxification pathway (Figure 1). It is therefore essential that the correct balance of activities of the antioxidant enzymes is maintained to ensure global cell protection.²¹ Our data confirm that the expression and activities of the principal antioxidant enzymes increase with gestational age, and that this is probably in response to the changes in maternal blood flow. Attempts were made to separate the activities of Cu/Zn and MnSOD using sodium cyanide to block the cytoplasmic enzyme, but as highly inconsistent results were obtained this proved not to be possible. Previous work using a native polyacrylamide gel electrophoresis activity gel indicated an increase in activity of both enzymes with gestational age,¹² and this is supported by the mRNA data reported here. Two splice variants were detected for MnSOD, and in human cell lines it has been demonstrated that the 4-kb variant is the more rapidly responsive of the two.²² This variant showed the greater differences with gestational age in our samples, although the differences failed to reach statistical significance. Our results are therefore in general agreement with the findings of Takehara et al²³ who reported an increase in placental total SOD and catalase activity from 5 weeks of gestation to term. It is pertinent that from their scattergrams it appears that most of the increase occurred toward the end of the first trimester.

If free radical generation exceeds the capacity of the antioxidant defenses then oxidative stress results. In this situation indiscriminate damage to proteins, lipids, and DNA can occur, leading to a loss of cell function. Recent work has confirmed that the protein deformations caused by oxidative stress induce the expression of Hsps in a similar manner to hyperthermia.¹³ Oxidative modification of protein thiol groups causes thermal stable proteins to become destabilized and to undergo thermal denaturation at physiological temperatures. The resultant molten-globule intermediates cause trimerization of the transcription factor Hsf-1, which confers DNA binding activity, so leading to gene activation. Hsps act as molecular chaperones to sequester damaged proteins, giving them an opportunity to refold or directing them to proteolytic pathways. Their expression represents an adaptive response aimed at preventing the aggregation of denatured proteins within the cytosol, and overexpression of both the constitutive and inducible forms of Hsp 70 confers increased resistance to oxidative stress in cell lines.²⁴ The peak of Hsp 70 expression we observed within the syncytiotrophoblast at 8 to 9 weeks therefore provides a sensitive marker of oxidative stress occurring *in vivo*.

This conclusion is further supported by the concurrent detection of elevated concentrations of nitrotyrosine residues. Although $O_2^{\cdot-}$ is rapidly dismutated by SOD, it also reacts avidly with nitric oxide to form peroxynitrite, a potent oxidant capable of initiating lipid peroxidation and nitrating tyrosine residues on a variety of proteins. This can lead to inactivation of enzyme activity, as for example has been demonstrated for MnSOD.²⁵ Because peroxynitrite has a relatively long half-life (~1 second) and is

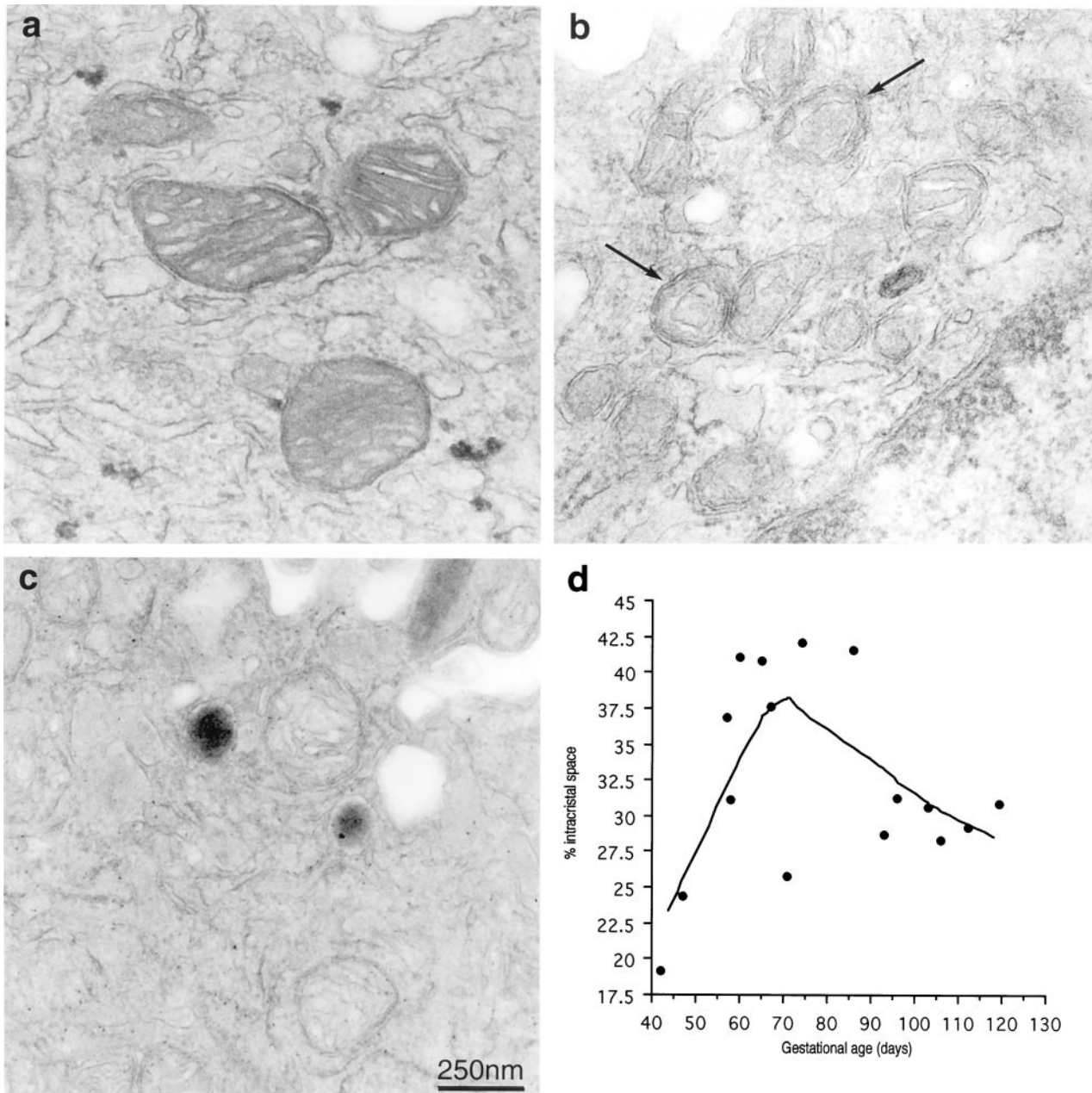


Figure 8. Electron micrographs of syncytiotrophoblastic mitochondria (arrows) at different gestational ages demonstrating the distortion of the cristae and dilatation of the intracristal space that coincides with Hsp 70 expression and the formation of nitrotyrosine residues at 6 weeks (a), 10 weeks (b), 14 weeks (c). **d:** Scattergram plot of the percentage mitochondrial volume occupied by intracristal space at different gestational ages. The line was fitted using the LOWESS technique with a tension of 66.

freely diffusible through biological membranes its potential targets are widespread.

The syncytiotrophoblast is particularly vulnerable to oxidative stress for two reasons. Firstly, because of its location on the villous surface this tissue will be the first to experience the increase in intervillous PO_2 , and so will be the principal beneficiary in terms of aerobic respiration. Secondly, we have previously shown that the syncytiotrophoblast contains much lower concentrations of the antioxidant enzymes than other villous tissues during early gestation.^{12,26,27} Low levels of MnSOD will place the mitochondria at particular risk of $O_2^{\cdot-}$ -mediated damage.

It has been known for many years that the ultrastructural morphology of mitochondria changes reversibly according to their metabolic activity.²⁸ The orthodox appearances of interdigitating cristae seen during periods of low oxygen consumption reflect a low respiration rate. By contrast, high respiration rates are associated with a reduction in volume, condensation of the matrix, and an increase in the intracristal space. On this basis, our findings are consistent with a general switch from anaerobic to aerobic metabolism within the syncytiotrophoblast at the end of the first trimester. The boundary between normal metabolic changes and damage resultant on ox-

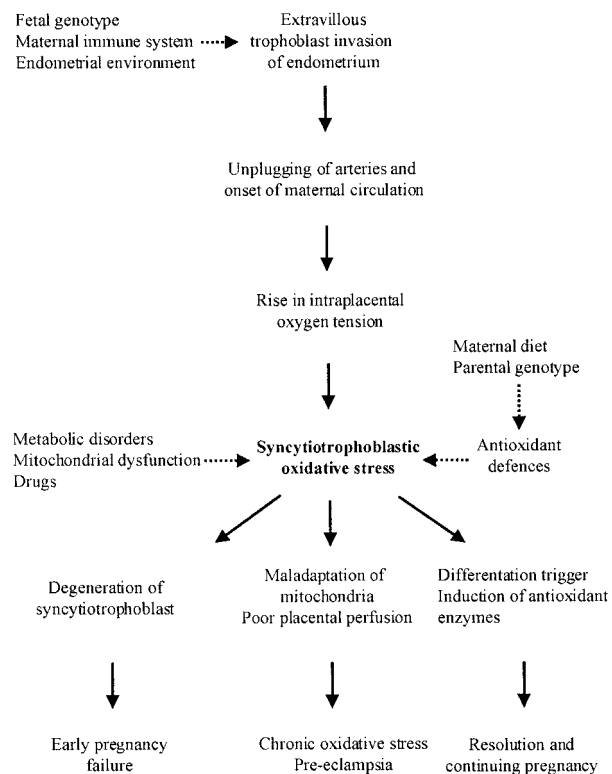


Figure 9. Summary diagram illustrating the origin and possible effects of the syncytiotrophoblastic oxidative stress. Factors that may modulate the degree of stress are indicated by the **dashed lines**.

oxidative stress is not clear however, and they may represent different stages along a gradual spectrum. For example, the cytotoxic action of tumor necrosis factor is mediated through increased free radical generation within mitochondria, and is associated with disruption of their cristae and loss of enzyme function.²⁹ The circular arrangements of cristae we observed at 9 to 10 weeks may represent early stages in the formation of the onion-skin whorls induced by tumor necrosis factor, indicating a degree of oxidative stress. We have previously observed qualitatively similar changes in mitochondrial morphology in villi maintained under 21% oxygen, where they are accompanied by loss of enzyme activity and of mitochondrial membrane potential as evidenced by rhodamine-123 fluorescence.^{12,30} It is likely therefore that mitochondrial function is impaired during onset of the maternal circulation, although clearly the situation is recoverable as our samples represent snapshots of what would otherwise have been normal on-going pregnancies. We suggest this may be a period of rapid mitochondrial turnover, with the formation of new mitochondria equipped with elevated concentrations of antioxidant defenses to cope with the increasing oxygen tension.

Overall therefore, it would seem that the onset of the full maternal arterial circulation to the placenta is associated with a transient period of placental oxidative stress in normal pregnancies (Figure 9). We hypothesize that this is because of a temporary imbalance between increased generation of free radical species as a result of the rapidly rising oxygen tension, and adaptations in the

antioxidant defenses to quench them. This burst of stress may serve an important physiological function in normal placental development by triggering differentiation pathways.^{31,32} For example, it may switch cytotrophoblast cells from a proliferative to an invasive phenotype, so stimulating the migration of extravillous trophoblast into the endometrium where they play a key role in the conversion of the spiral arteries.^{33–35} Failure of this process is associated with pre-eclampsia, a common complication of pregnancy associated with poor perfusion of the placenta and chronic oxidative stress.^{36,37}

Equally, however, it may have potentially very damaging effects if the placental oxidative stress should become too great and trophoblastic degeneration occurs as it does *in vitro* (Figure 9).^{12,38} Oxidation of thiol groups on proteins incorporated in the inner mitochondrial membrane is thought to promote the mitochondrial permeability transition through opening of the BCL-2 regulated mega-channel. Loss of ionic gradients and the release of small proteins such as cytochrome c into the cytoplasm may result in activation of the caspase cascade and hence apoptosis.³⁹ Enzymes located in the matrix and on the inner membrane, including those of the respiratory chain, will also be vulnerable through direct oxidation, but in addition the peroxidation of the membrane lipids can significantly impair their function.^{25,40,41} If sufficiently severe these changes lead to depletion of adenosine triphosphate stores, and may cause cells to undergo either necrosis or apoptosis.

Because the syncytiotrophoblast is responsible for all placental hormone synthesis and active transport,⁴² pregnancy failure would rapidly ensue. The magnitude of the stress will depend on the rate of increase in PO₂ within the intervillous space, and on the state of the placental antioxidant defenses (Figure 9). In cases of inevitable ongoing miscarriage and of missed abortion there is premature and excessive entry of maternal blood into the intervillous space.^{9,43} Histological examination of the decidua in such cases reveals that trophoblast invasion is less extensive than normal, and that plugging of the apical portions of the spiral arteries by endovascular aggregations of cytotrophoblast cells is incomplete.⁴⁴ Hence, the onset of the maternal circulation is likely to have been precipitate. Placental tissues are most susceptible to lipoperoxidation at 7 weeks of gestational age,²³ and this will be further exacerbated if antioxidant defenses are depleted. It has been suggested that women with low concentrations of serum selenium, the transition metal embedded within GPX, experience a higher rate of early pregnancy failure, although this was not confirmed by a recent case-controlled study.^{45,46} It has also been reported that mice deficient in glucose-6-phosphate dehydrogenase, an enzyme involved in maintaining the available pool of reduced glutathione, show a higher rate of intrauterine deaths and fetal resorptions than controls.⁴⁷ There may be a human corollary to this phenomenon, for the incidence of G6PD-deficient $-/\gamma$ males and $-/-$ females born among all G6PD-deficient groups in Europe is >50% lower than expected.⁴⁸ These data suggest a lower survival rate than expected for the affected embryos. Oxidative stress of the syncytiotrophoblast may

therefore act as the final common pathway for a number of diverse conditions associated with early pregnancy failure.

Acknowledgments

The confocal and electron microscopy was performed in the Multimaging Center of the School of Biological Sciences, University of Cambridge, which was established through a generous grant from the Wellcome Trust.

References

1. Boyd JD, Hamilton WJ: The Human Placenta. Cambridge, Heffer and Sons, 1970
2. Larsen WJ: Human Embryology. New York, Churchill Livingstone, 1997
3. Hustin J, Schaaps JP: Echographic and anatomic studies of the maternotrophoblastic border during the first trimester of pregnancy. *Am J Obstet Gynecol* 1987, 157:162–168
4. Hustin J, Schaaps JP, Lambotte R: Anatomical studies of the uteroplacental vascularisation in the first trimester of pregnancy. *Troph Res* 1988, 3:49–60
5. Jauniaux E, Jurkovic D, Campbell S: Current topic: in vivo investigation of the placental circulations by Doppler echography. *Placenta* 1995, 16:323–331
6. Moll W: Invited commentary: absence of intervillous blood flow in the first trimester of human pregnancy. *Placenta* 1995, 16:333–334
7. Jaffe R, Jauniaux E, Hustin J: Maternal circulation in the first-trimester human placenta—myth or reality? *Am J Obstet Gynecol* 1997, 176:695–705
8. Kurjak A, Kupesic S, Hafner T, Kos M, Kostovic-Knezevic L, Grbesa D: Conflicting data on intervillous circulation in early pregnancy. *J Perinat Med* 1997, 25:225–236
9. Jauniaux E, Zaidi J, Jurkovic D, Campbell S, Hustin J: Comparison of colour Doppler features and pathologic findings in complicated early pregnancy. *Hum Reprod* 1994, 9:243–247
10. Valentin L, Sladkevicius P, Laurini R, Söderberg H, Marsal K: Uteroplacental and luteal circulation in normal first-trimester pregnancies: Doppler ultrasonographic and morphologic study. *Am J Obstet Gynecol* 1996, 174:768–775
11. Freeman BA, Crapo JD: Hyperoxia increases oxygen radical production in rat lungs and lung mitochondria. *J Biol Chem* 1981, 256:10986–10992
12. Watson AL, Skepper JN, Jauniaux E, Burton GJ: Susceptibility of human placental syncytiotrophoblastic mitochondria to oxygen-mediated damage in relation to gestational age. *J Clin Endocrinol Metab* 1998, 83:1697–1705
13. Freeman ML, Borrelli MJ, Meredith MJ, Lepock JR: On the path to the heat shock response: destabilization and formation of partially folded protein intermediates, a consequence of protein thiol modification. *Free Radic Biol Med* 1999, 26:737–745
14. Jauniaux E, Watson AL, Ozturk O, Quick D, Burton GJ: In-vivo measurement of intrauterine gases and acid-base values early in human pregnancy. *Hum Reprod* 1999, 14:2901–2904
15. Cowan DB, Weisel RD, Williams WG, Mickle DAG: Identification of oxygen responsive elements in the 5'-flanking region of the human glutathione peroxidase gene. *J Biochem* 1993, 268:26904–26910
16. Chandrasekar B, Colston JT, Freeman GL: Induction of proinflammatory cytokine and antioxidant enzyme gene expression following brief myocardial ischaemia. *Clin Exp Immunol* 1997, 108:346–351
17. Hamilton WJ, Boyd JD: Development of the human placenta in the first three months of gestation. *J Anat* 1960, 94:297–328
18. Harris JWS, Ramsey EM: The morphology of human uteroplacental vasculature. *Contrib Embryol* 1966, 38:43–58
19. Burton GJ, Jauniaux E, Watson AL: Maternal arterial connections to the placental intervillous space during the first trimester of human pregnancy; the Boyd Collection revisited. *Am J Obstet Gynecol* 1999, 181:718–724
20. Chance B, Sies H, Boveris A: Hydroperoxide metabolism in mammalian organs. *Physiol Rev* 1979, 59:527–605
21. Michiels C, Raes M, Toussaint O, Remacle J: Importance of S-glutathione peroxidase, catalase, and Cu/Zn-SOD for cell survival against oxidative stress. *Free Radic Biol Med* 1994, 17:235–248
22. Melendez JA, Baglioni C: Differential induction and decay of manganese superoxide-dismutase messenger-RNAs. *Free Radic Biol Med* 1993, 14:601–608
23. Takehara Y, Yoshioka T, Sasaki J: Changes in the levels of lipoperoxide and antioxidant factors in human placenta during gestation. *Acta Med Okayama* 1990, 44:103–111
24. Su C-Y, Chong K-Y, Owen OE, Dillmann WH, Chang C, Lai C-C: Constitutive and inducible hsp70s are involved in oxidative resistance evoked by heat shock or ethanol. *J Mol Cardiol* 1998, 30:587–598
25. Yamakura F, Taka H, Fujimura T, Murayama K: Inactivation of human manganese-superoxide dismutase by peroxynitrite is caused by exclusive nitration of tyrosine 34 to 3-nitrotyrosine. *J Biol Chem* 1998, 273:14085–14089
26. Watson AL, Palmer ME, Jauniaux E, Burton GJ: Variations in expression of copper/zinc superoxide dismutase in villous trophoblast of the human placenta with gestational age. *Placenta* 1997, 18:295–299
27. Watson AL, Skepper JN, Jauniaux E, Burton GJ: Changes in the concentration, localisation and activity of catalase within the human placenta during early gestation. *Placenta* 1998, 19:27–34
28. Hackenbrock CR: Ultrastructural bases for metabolically linked mechanical activity in mitochondria. 1. Reversible ultrastructural changes with change in metabolic steady state in isolated liver mitochondria. *J Cell Biol* 1966, 30:269–297
29. Schulze Osthoff K, Bakker AC, Vanhaesebroeck B, Beyaert R, Jacob WA, Fiers W: Cytotoxic activity of tumor necrosis factor is mediated by early damage of mitochondrial functions. Evidence for the involvement of mitochondrial radical generation. *J Biol Chem* 1992, 267:5317–5323
30. Watson AL, Skepper JN, Jauniaux E, Burton GJ: Reducing oxidative stress effects in early human placental villi during in vitro culture. *Placenta* 1999, 20:A69
31. Sun Y, Oberley LW: Redox regulation of transcriptional activators. *Free Radic Biol Med* 1996, 21:335–348
32. Arrigo A-P: Gene expression and the thiol redox state. *Free Radic Biol Med* 1999, 27:936–944
33. Genbacev O, Joslin R, Damsky CH, Polliotti BM, Fisher SJ: Hypoxia alters early gestation human cytotrophoblast differentiation/invasion in vitro and models the placental defects that occur in preeclampsia. *J Clin Invest* 1996, 97:540–550
34. Caniggia I, Mostachfi H, Winter J, Gassmann M, Lye SJ, Kuliszewski M, Post M: Hypoxia-inducible factor-1 mediates the biological effects of oxygen on human trophoblast differentiation through TGFbeta(3). *J Clin Invest* 2000, 105:577–587
35. Kam EP, Gardner L, Loke YW, King A: The role of trophoblast in the physiological change of decidual spiral arteries. *Hum Reprod* 1999, 14:2431–2438
36. Roberts JM, Hubel CA: Is oxidative stress the link in the two-stage model of pre-eclampsia? *Lancet* 1999, 354:788–789
37. Wang Y, Walsh SW: Placental mitochondria as a source of oxidative stress in pre-eclampsia. *Placenta* 1998, 19:581–586
38. Palmer ME, Watson AL, Burton GJ: Morphological analysis of degeneration and regeneration of syncytiotrophoblast in first trimester villi during organ culture. *Hum Reprod* 1997, 12:379–382
39. Kowaltowski AJ, Vercesi AE: Mitochondrial damage induced by conditions of oxidative stress. *Free Radic Biol Med* 1999, 26:463–471
40. Du G, Mouithys-Mickalad A, Sluse FE: Generation of superoxide anions by mitochondria and impairment of their functions during anoxia and reoxygenation in vitro. *Free Radic Biol Med* 1998, 25:1066–1074
41. Cardoso SM, Pereira C, Oliveira CR: Mitochondrial function is differentially affected upon oxidative stress. *Free Radic Biol Med* 1999, 26:3–13
42. Kaufmann P, Burton GJ: Anatomy and Genesis of the Placenta. The Physiology of Reproduction. Edited by E Knobil, JD Neill. New York, Raven Press, 1994, pp 441–484
43. Schwärzler P, Holden D, Nielsen S, Hahlin M, Sladkevicius P, Bourne TH: The conservative management of first trimester miscarriages and the use of colour Doppler sonography for patient selection. *Hum Reprod* 1999, 14:1341–1345

44. Hustin J, Jauniaux E, Schaaps JP: Histological study of the materno-embryonic interface in spontaneous abortion. *Placenta* 1990, 11:477-486
45. Barrington JW, Lindsay P, James D, Smith S, Roberts A: Selenium deficiency and miscarriage: a possible link? *Br J Obstet Gynaecol* 1996, 103:130-132
46. Nicoll AE, Norman J, Macpherson A, Acharya U: Association of reduced selenium status in the aetiology of recurrent miscarriage. *Br J Obstet Gynaecol* 1999, 106:1188-1191
47. Nicol CJ, Zielenski J, Tsui L-C, Wells PG: An embryoprotective role for glucose-6-phosphate dehydrogenase in developmental oxidative stress and chemical teratogenesis. *FASEB J* 2000, 14:111-127
48. Sodeinde O: Glucose-6-phosphate dehydrogenase deficiency. *Baill Clin Hematol* 1992, 5:367-382